

Non-destructive Inspection System Development for Secondary Battery Welding Part

K. Chun

Department of Electronic Engineering, Daegu Catholic University, Gyeongsan, Gyeongbuk, Korea

Article Info

Article history:

Received Sep 24, 2022

Revised Dec 3, 2022

Accepted Dec 15, 2022

Keyword:

Non-destructive
AOI
Secondary Battery
Welding

ABSTRACT

In this paper, we develop a non-destructive inspection system for secondary battery welding. In a secondary battery, when the insulation or separator of each electrode is damaged by an impact from the outside depending on the degree of welding, an internal short circuit occurs during charging and fires even if it does not ignite at that time. To detect this, a non-destructive AOI (Automatic Optical Inspection) system is developed that compares the inspection target with the reference image to determine whether there is a proper indentation in the welding part. The system consists of a precision alignment stage on the lower part and imaging equipment that performs AOI, a non-destructive inspection on the upper part. And the appropriate exposure, i.e., the aperture setting of the used camera, was confirmed through the experiment according to the position of the pole.

Copyright © 2018 Institute of Advanced Engineering and Science.
All rights reserved.

Corresponding Author:

K. Chun,
Department of Electronic Engineering,
Daegu Catholic University,
Gyeongsan, Gyeongbuk, Korea
Email: kchun@cu.ac.kr

1. INTRODUCTION

In secondary batteries, lithium batteries are the most widely used among secondary batteries because of their high volumetric energy density and good charging efficiency. Kinds of lithium batteries are lithium-ion battery and lithium polymer battery, and there is no essential difference, but only difference is the liquid state or the gel-like solid polymer in the electrolyte. And lithium batteries are widely used around us so much that they cannot be separated from our lives, such as cell phones, cameras, drones, auxiliary batteries for black boxes for vehicles, electric vehicles, and electric storage systems (ESS). Lithium batteries can cause fires if improperly designed, manufactured, and handled, and in fact, significant fires related to lithium batteries are occurring.

This kind of lithium battery can also have ignition mechanisms depending on various situations, and among them, the influence of the welding degree in particular is one of the causes that cannot be ignored. If the insulation or separator of each electrode is damaged by an impact from the outside depending on the degree of welding, an internal short circuit may occur and ignition may occur during charging after the damage even if the ignition does not occur at that time. Therefore, contact destructive testing is applied because it is impossible to directly check the welding degree of welding, which has an important effect on the charge and discharge performance of the battery as well as the prevention of safety accidents. In other words, it is a problem that occurs after time passes, it also affects the quality of the product.

The post-process inspection methods include eddy current, ultrasonic, visual, or radiographic testing techniques [1-7]. But vision-based technique, including a 3D vision-based measuring approach under structured lighting, may be best suited to on-line inspection for welding joints than other methods, such as two-dimensional array ultrasonic detection [8] and X-ray testing [9] because they are expensive. These presented vision-based techniques can not be adopted directly to deal with the quality assessment for the Li-

ion welding joints due to their nearly different scenario which results in the different technique bottlenecks. But vision-based approaches used in IC solder joint inspection may be used or studied for the welding joint inspection.

Based on many types of features extracted from multi-color solder joint images under tier lighting, classifier-based methods, such as support vector machine (SVM) by Wu [10], feature-based method, such as shape digital logistic (SDL) by Wu and Zhang [11], statistical modeling-based method, such as an improved visual background extraction (ViBe) by Cai [12], and deep learning-based method, were presented for IC solder joint inspection. But these vision-based methods all based on color features under complex multi-angle and multi-color lighting. This kind of lighting configuration is expensive and can not generate meaningful features for Li-ion battery welding joints due to their shape irregularities.

In this paper, we develop a non-destructive inspection system for secondary battery welding. Basically, the system consists of a precision alignment stage on the lower part and imaging equipment that performs AOI, a non-destructive inspection on the upper part. The indentation inspection is performed using the image obtained from the camera, and the pass/fail of the product is determined whether the product is a fake or not according to the determination algorithm. At this time, the algorithm can apply the different discrimination method according to the welding method and set the demand-based ROI (Region of Interest) area. And the appropriate exposure according to the position of the pole was confirmed through the experiment.

2. NON-DESTRUCTIVE INSPECTION SYSTEM

2.1. Secondday Battery and Welding

Secondday Battery

The secondary battery refers to a battery that can be reused through charging even after being discharged and means a device that converts external electrical energy into chemical energy, stores it, and generates electricity when needed.

Primary batteries are batteries that cannot be recharged and reused. There are normal batteries and alkaline batteries that are frequently used in daily life. Secondary batteries include lead-acid batteries, nickel-cadmium batteries (NiCd), nickel-metal hydride batteries (Ni-MH), lithium ion batteries (Li-ion), and lithium ion polymer batteries (Li-ion polymer). Secondary batteries provide both economic and environmental advantages compared to primary batteries that are used and discarded once and are produced and sold in standard AA, AAA, C, sub_C, D, 9 volt standards.

Lithium batteries are made in a cylindrical shape filled with electrolyte by winding a copper plate and an aluminum plate, a square shape which a continuous copper plate, a separator, and an aluminum plate are stacked on top of each other, and other square type which a cut rectangular copper electrode plate, a separator, and an aluminum electrode plate are laminated.

When electronic products are connected to the battery (discharging), lithium ions (Li⁺) in the graphite lattice structure of the negative electrode begin to move into the crystal structure of the positive electrode through the separator, and in this process, electrons (e⁻) ride the wire as it moves from the cathode to the anode, current flows from the anode to the cathode, and when charging, the lithium ions (Li⁺) intercalated in the metal oxide are directed back toward the cathode.

Welding

Ultrasonic welding is a typical method for applying welding when joining electrodes of such secondary batteries. Ultrasound is an elastic wave that can propagate in various material media (gas, liquid, solid). Because ultrasonic waves have a short wavelength and can form the speed of sound, not only can the entire energy of ultrasonic waves be focused in a required direction, but also can ultrasonic radiation, that is, the total energy of the emitter be focused in a small volume. A negative lens that plays this role is shaped very much like an optical lens (the principle of ultrasonic welding).

Using these ultrasonic characteristics, the principle of ultrasonic welding is summarized as follows.

- Due to the property of ultrasonic waves, it is difficult to focus ultrasonic waves of low frequency (15,000 to 60,000 Hz). However, it is possible in some cases.

- In the physical process of ultrasonic energy focusing, assuming that the sound wave propagates inside a very thin and long metal rod at the tip, the cross-sectional area of the rod becomes smaller and smaller, so the output (sound intensity) passing through the unit cross-sectional area will gradually increase.

- According to the calculation, the most effective shape of the rod is the exponentially changing shape and the step shape. If the length of the rod is selected to be 1, 2 or 3 wavelengths, the concentration effect can be further improved. In the resonant system, the strength at the end of the horn, that is, the vibration amplitude, can be raised to the limit of the strength of the material.

Therefore, in ultrasonic welding, if two metal sheets are put together and high-frequency vibration is applied equally to the contact surface on one side, they are joined in a short time. First, it is because the oxide layer on the free surface of the metal is removed by strong friction. Second, the surface of the metal is strongly heated by friction, and the joint is formed by softening.

Even when heated, the heating is limited to the surface part and not the other parts, so ultrasonic welding is called cold welding. To summarize the characteristics of ultrasonic welding, it is a type of solid-state welding and is a method of welding by locally applying high-frequency vibration energy and pressure during welding.

A characteristic of ultrasonic welding is the piezoelectric effect. This means the mutual conversion of mechanical energy and electrical energy through the piezoelectric body. Vibration can be applied using this mechanical energy. As a kind of solid state welding, it is characterized in that a sound metallurgical joint is obtained without melting the base material by applying local high-frequency vibration energy and pressure during welding.

In ultrasonic welding, it is indirectly proved that the surface to be welded does not need to be cleaned in advance because the pressure and vibration force act at the same time, and that cleaning occurs naturally in the stage before welding. Ultrasonic welding is a method of welding using the effect that the boundary lines of the separated surface layers are reconnected after the oxide films of different welding objects are removed.

The configuration of the ultrasonic welding device is shown in Figure 1. Ultrasonic vibration is generated by the transducer and this vibration is transmitted to the base material through the sonotrode. The acoustic electrode is in direct contact with the welding material, and vibration energy is transmitted through this electrode, and the clamping force during welding is applied at the end of the acoustic electrode. Anvil supports the welding material and serves to add a reaction force to the pressing force.

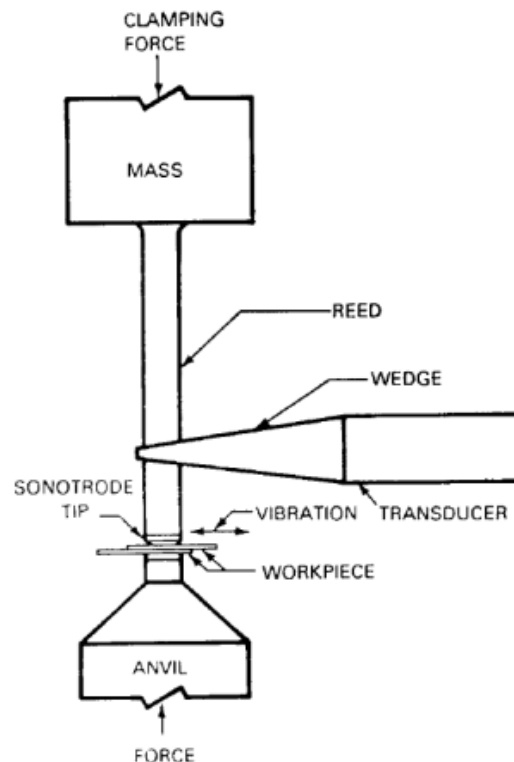


Figure 1. Basic diagram of ultrasonic welding

2.2. Inspection System

For secondary batteries, the proposed facility detects welding indentations using a non-destructive inspection method through application of computer vision and algorithm after ultrasonic welding of electrode parts of secondary batteries. The concept diagram of the facility is shown in Figure 2.

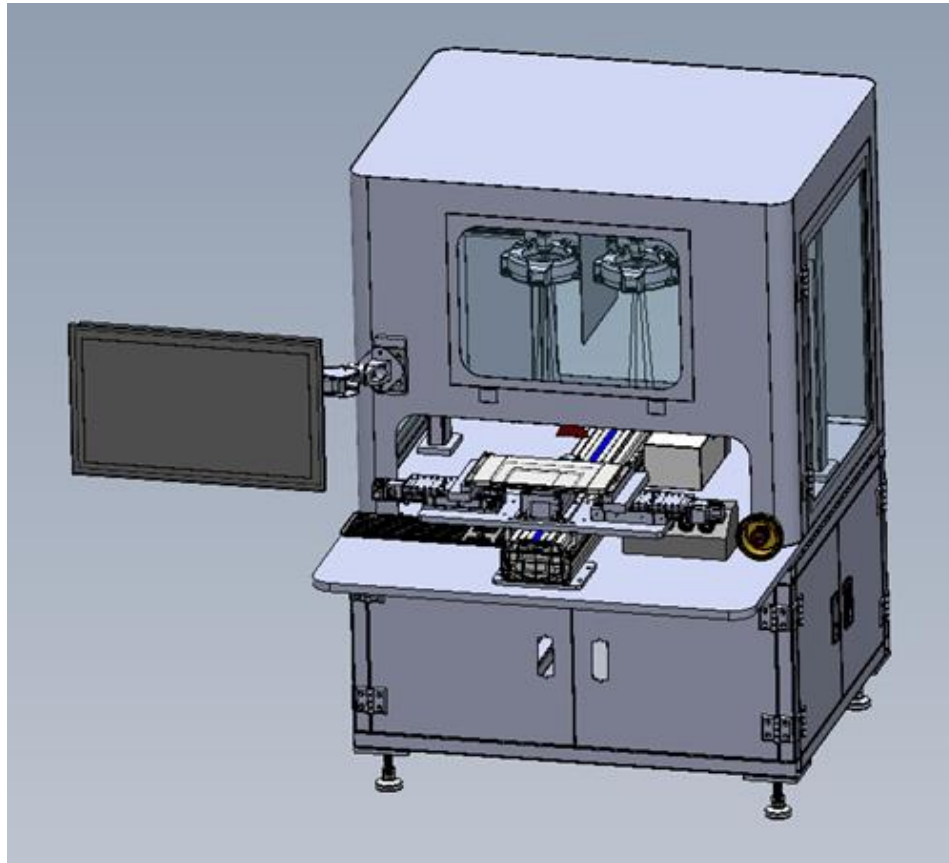


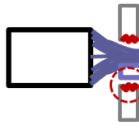
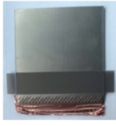
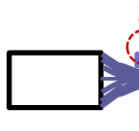
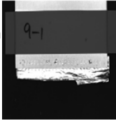
Figure 2. Secondary battery welding part non-destructive inspection equipment

The system specifications are as follows.

Description	Specification
System Size	▷ Size : L 1,000 x W 1,200 x H 1,430 (mm) ※ Pass Line : 762 mm (±10)
Battery Size	▷ bi-direction /uni-direction

Figure 3. Size specifications of inspection system and battery

The detection surfaces are shown in Figure 4, and the developed equipment for the inspection is applied only to the products subject to ultrasonic welding. However, the application of the laser welding target product also can be possible after additional testing is carried out.

Detection Surface	Welding		Detection Surface		
	Ultrasonic Welding		Lead Back detection		▷ can be applied
	Laser Fusion		Lead Front detection		▷ not yet ※ same vision system, but different algorithm required

※ This equipment is developed only for "ultrasonic welding". However, for products subject to "laser fusion", additional tests will be conducted and it can be applied by updating the detection algorithm.

Figure 4. Detection surface

The detections from the video image of the inspection object are as follows.

No	Detection	Measurement
①	Indentation Size	area/width/height
②	ROI area	Area comparison of ROI left/middle/right within detection area

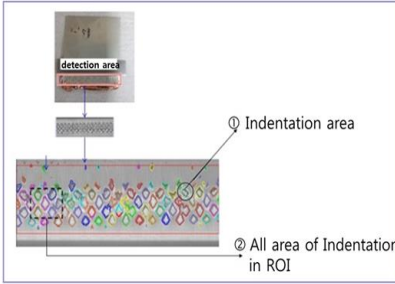


Figure 5. Detections

The work process is as follows.

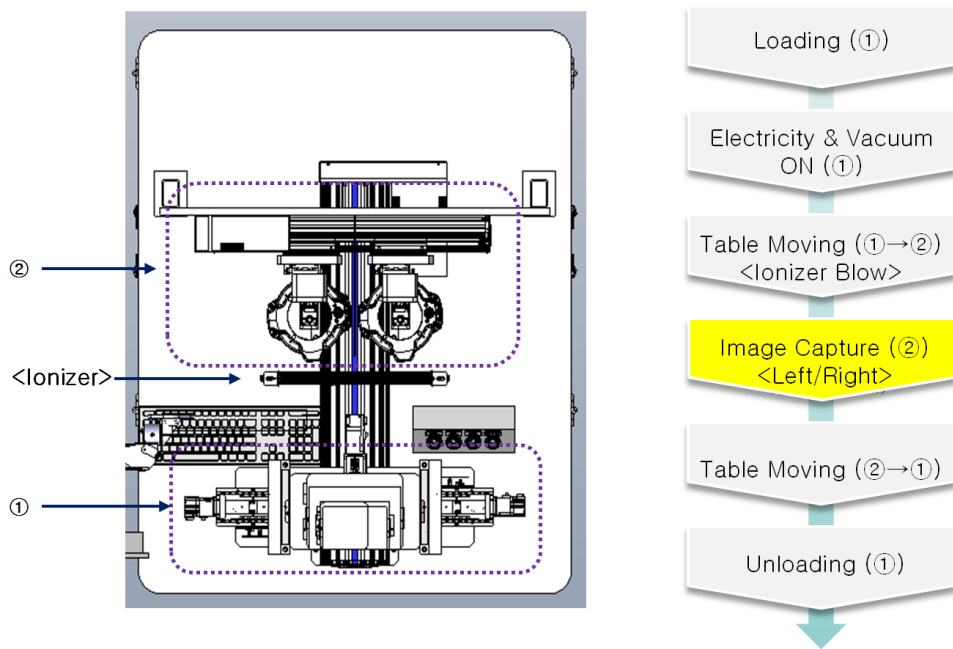


Figure 6. Work flow

The main units of the system are as follows.

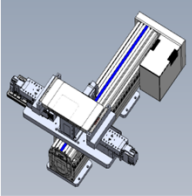
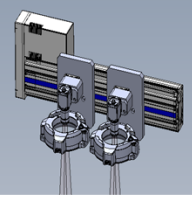
No	Unit	Figure	Configuration
1	Worktable Unit		<ul style="list-style-type: none"> Worktable : <ul style="list-style-type: none"> Motorized Type (Auto M/C) : X/Z Axis Porus Chuck is applied to deal with the lead crimping part Moving Axis : Orthogonal Robot
2	Camera Unit		<ul style="list-style-type: none"> Optic System : 2 Set Motorized Type with Centering (Auto M/C)

Figure 7. Main units

Depending on the battery type, the camera shooting method is set. If there are images of both indentations that are connected and operated in both directions (bidirectional type), the left/right camera acquires images by shooting. And in the case of batteries that are connected and operated in only one direction (unidirectional type), the welding parts are photographed using only the left camera. The first welding part is photographed and then moved and acquired the photo of the second welding part.

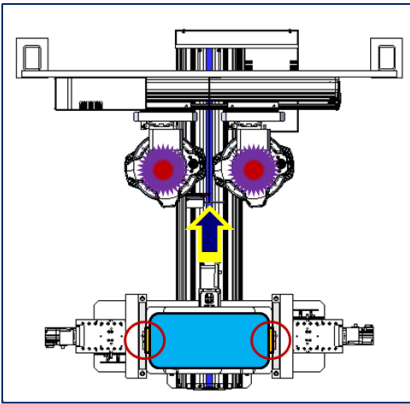
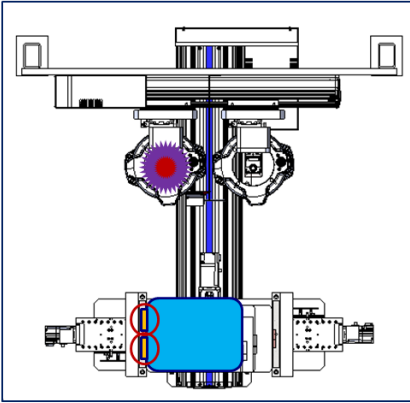
No	Type	Flow	Description
1	Bi-direction		<ul style="list-style-type: none"> Moving for photo shooting after safe arrival on the table Lead photographing for left/right camera
2	Uni-direction		<ul style="list-style-type: none"> Moving for photo shooting after safe arrival on the table Left camera only works 1st Lead photographing <ul style="list-style-type: none"> → Worktable Y-axis Moving → 2nd Lead photographing

Figure 8. Photographing ways for each battery types

In computer vision for non-destructive inspection of such a welding part, imaging equipment specifications for precise image shooting are also important, and the system used is as follows.

Item	Spec
Camera	Area Camera / 10M
Lens	FA3501C
Image resolution	15um/pixel
Magnification	0.11x
FOV	57.6mm × 41.2mm
Working distance	about 333mm
Low Working distance	about 246mm
DOF	about 1.2mm
Illuminator	LED Blue Dome(Φ140)

Figure 9. Vision system specifications

The algorithm for determining whether the welding part is indented with this non-destructive AOI inspection system is as follows. First, a region of interest (ROI), which is a region of interest indicated by a red rectangle in the figure below, is designated and the indentation is determined using the image of the ROI region. After obtaining the size of the indentation area in the ROI area, the ratio of the size of the indentation area to the entire ROI area is applied as a criterion of good welding or not. Depending on the degree of conformity, if the manufacturing quality is defective, NG (Not Good) is displayed and the measured data is stored.

The captured ROI area is compared with the master image by extracting features after applying effective image enhancement for discrimination through pre-processing.

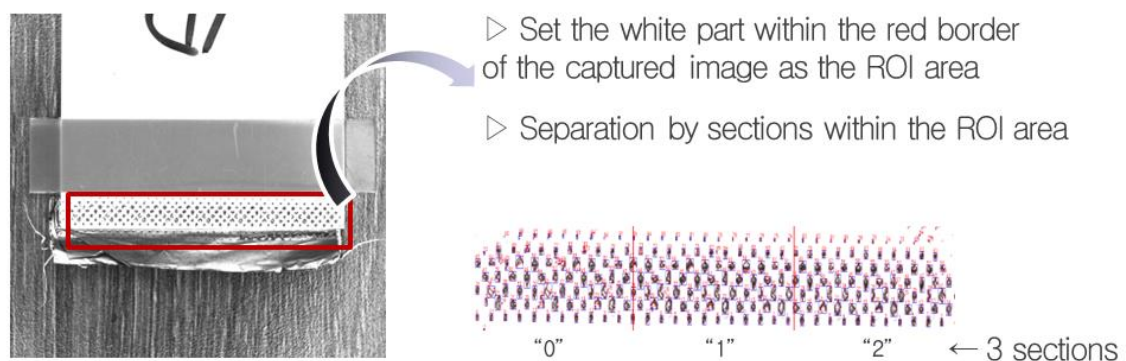


Figure 10. Inspection algorithm

3. TEST AND VALIDATION

The developed non-destructive testing system for the secondary battery welding part is in the Figure 11. Basically, the system has a stage that can be precisely aligned on the lower part and a camera imaging device that performs AOI, a non-destructive inspection, on the upper part. The inspection determines whether the product is a fake or not and the main components include DIC optical system for precise image measurement, automatic focusing using an auto focusing unit, and precise alignment using a linear moving axis stage and controller, and an image processing system for processing the acquired image.

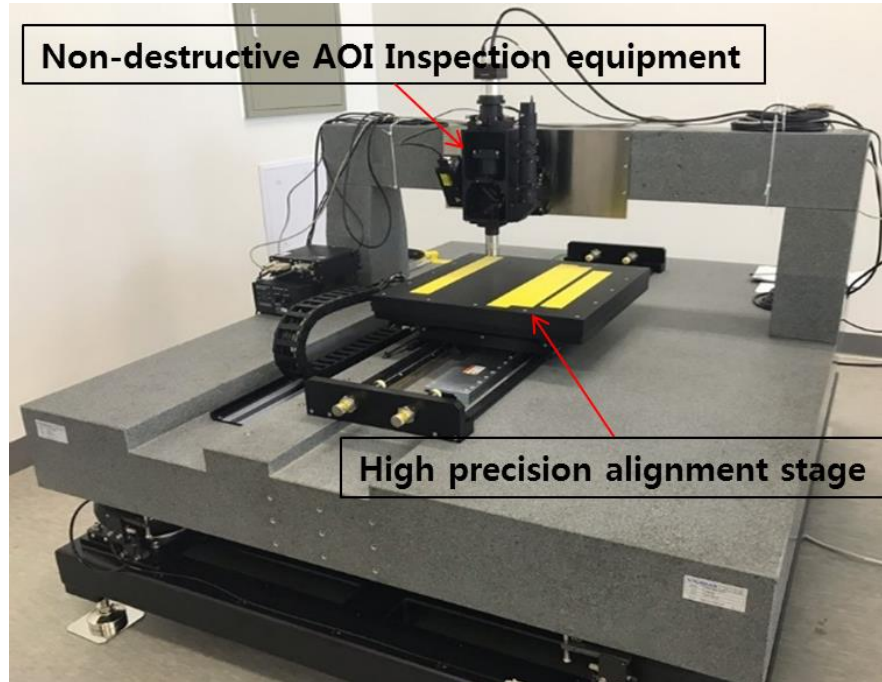


Figure 11. Non-destructive Inspection test bed for the secondary battery welding part

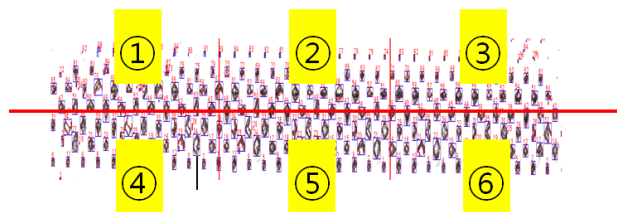
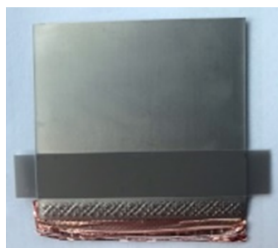
In the test 1 (3 samples) and 3 (4 samples) experiments, the recognition efficiency of indentation according to the change in welding strength and exposure value was confirmed. In the test 2 (2 samples) and 4 (2 samples) experiments, Check the difference in recognition efficiency according to changes in the location of the recognition area (Left, Center, Right) and exposure values.

For non-destructive AOI inspection, the welding part scan area is divided as 6 sections, and this is a method that reflects the needs of actual users.

■ Inspection info

Inspection	Details
machine	No. 3
model	S20P
anode/cathode	cathode

■ Sections



■ Data

Data	Section	Total (Sum of ①~⑥)	Left (①+④)	Middle (②+⑤)	Right (③+⑥)	Upper (①+②+③)	Lower (④+⑤+⑥)
	pixel ratio						

Figure 12. Welding data definition

And the area detection algorithm from the image applies two modes, and the methods are shown in Figure 13.

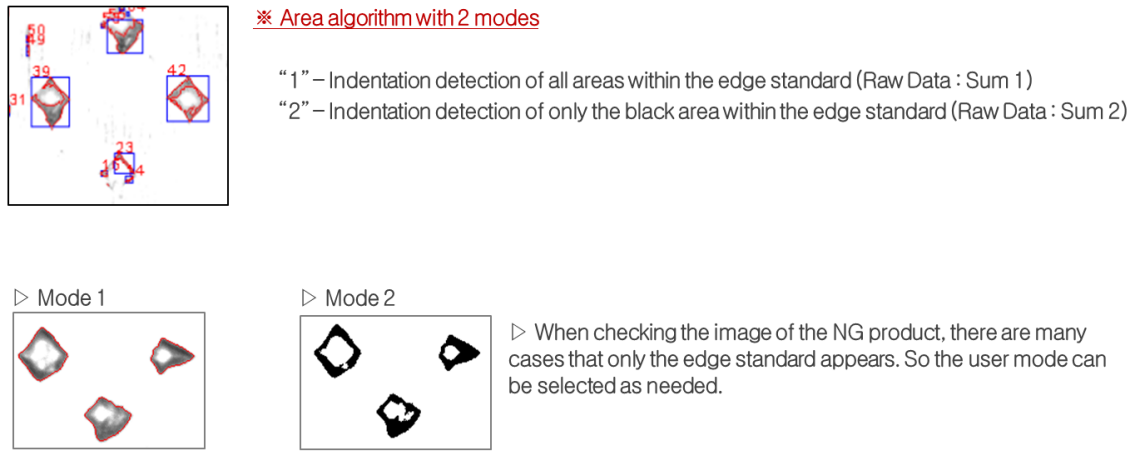


Figure 13. Detection mode

The test environments of test 1 are in the Figure 14. First, Test 1 (positive electrode) was performed according to the welding weak condition (10-30 kgf) and the strong condition (50-60 kgf).

Pole	Exposure	Test group	Numbers	Welding
Anode(+)	2500 / 2700	1	3 EA	Weak (10~30kgf)
		2	3 EA	Strong (50~60kgf)
Result	▶ The difference is about twice when based on the indentation area			

Figure 14. Test 1(anode) – different welding conditions and exposure

If you look at the results below, there is a difference of about 2 times based on the indentation area. Two groups were tested with three products each, and the exposure levels were tested at 2500 and 2700.

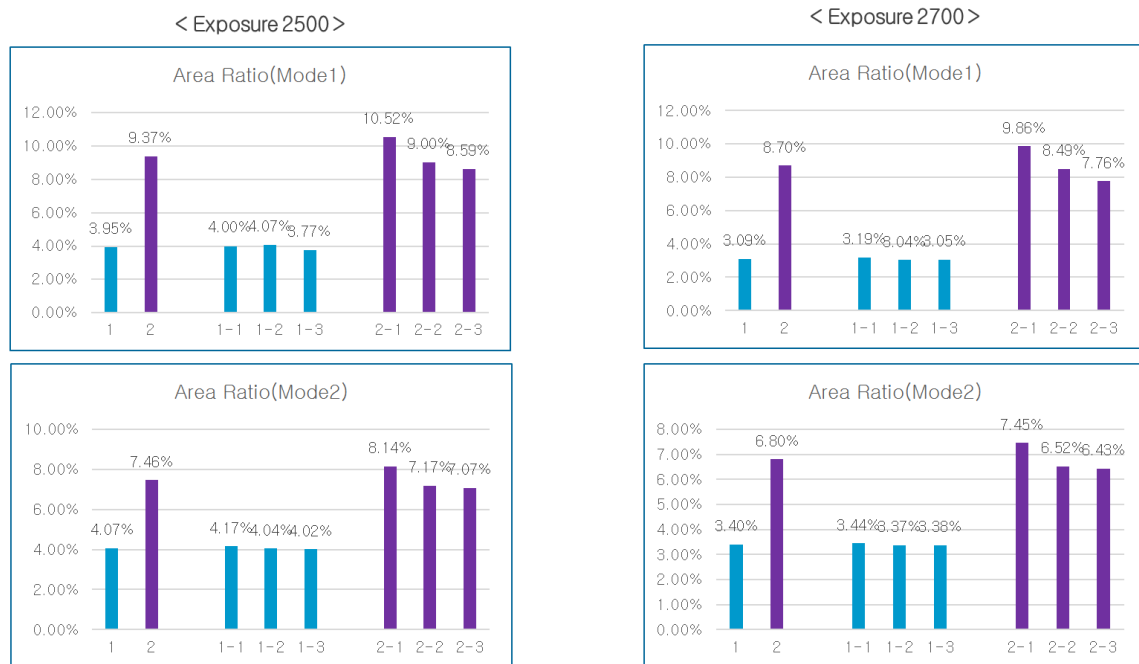


Figure 15. Results from welding and exposure (Test 1 - anode)

Next, test 2 (positive pole) was performed to check the tendency based on the horizontality for weak welding conditions and strong conditions. This is a test that confirms the result of the total area and the tendency for each reference location.

Pole	Exposure	Test group	Numbers	Horizontality	※ Locations
Anode(+)	2500	3	2 EA	Weak(260)	: 3 sections in the inspection area L – Left / C – Center / R – Right
		4	2 EA	Strong(280)	
Result	▶ Tendency in the horizontality is confirmed				

Figure 16. Test 2(anode) – tendency in the horizontality for strong/weak conditions

As a result of checking the weak welding condition and the strong condition by reference position in the horizontality standard, it was possible to confirm the same tendency in the case of the welding-intensive condition sample.

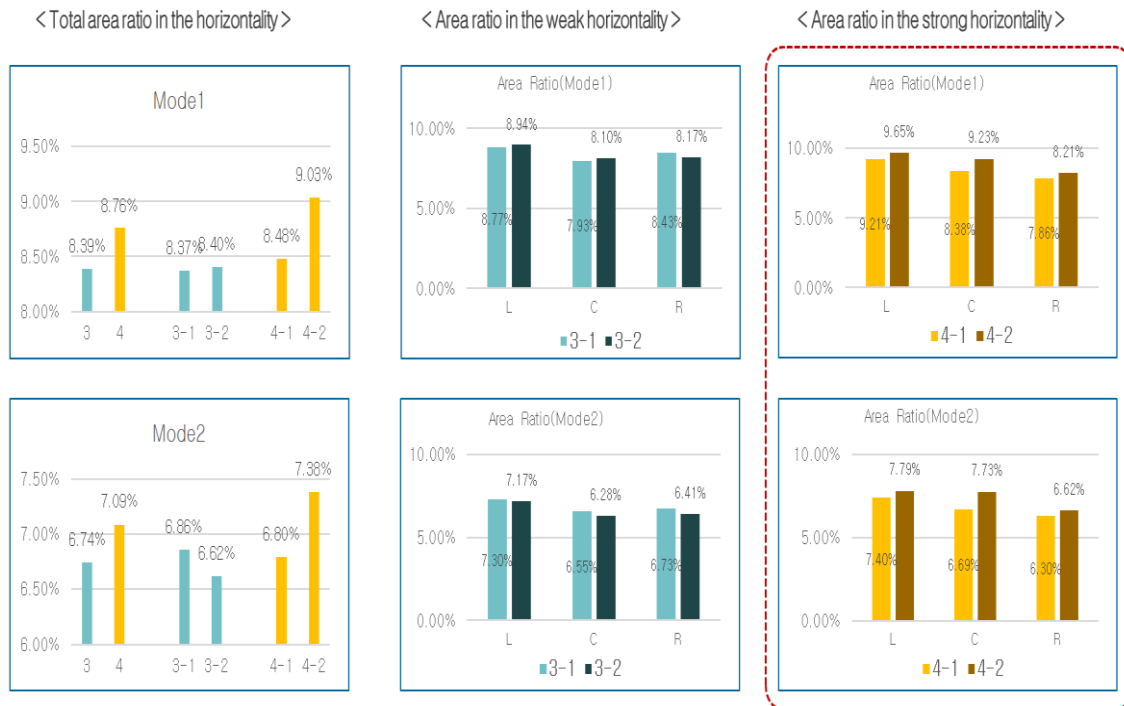


Figure 17. Results in the horizontality from welding (Test 2 - anode)

Test 3 was performed on the negative electrode under the same conditions as Test 1 (positive electrode).

Pole	Exposure	Test group	Numbers	Welding
Cathode(-)	4500 / 5000	5	4 EA	Weak (30~40kgf)
		6	4 EA	Strong (60~70kgf)
Result	▶ The difference is 1.7 times when based on the indentation area			

Figure 18. Test 3(cathode) – different welding conditions and exposure

However, at this time, each of the four samples was tested, and the exposure level was also different from the positive electrode, 4500 and 5000 were used. As a result of the test, there was a difference of about 1.7 times based on the indentation area according to the welding conditions, and the tendency was the same regardless of the degree of exposure.



Figure 19. Results from welding and exposure (Test 3 - cathode)

Test 4 applies the same situation as Test 2 to the negative pole.

Pole	Exposure	Test group	Numbers	Horizontality	* Locations : 3 sections in the inspection area L – Left / C – Center / R – Right
Cathode(-)	4500	7	2 ea	Weak(260)	
		8	2 ea	Strong(280)	
Result		▶ Tendency in the horizontality is confirmed			

Figure 20. Test 4(cathode) – tendency in the horizontality for strong/weak conditions

In this case, similar to Test 2, it can be confirmed that the result of the strong welding shows the same tendency of the entire area in the horizontality standard at the reference position as well.

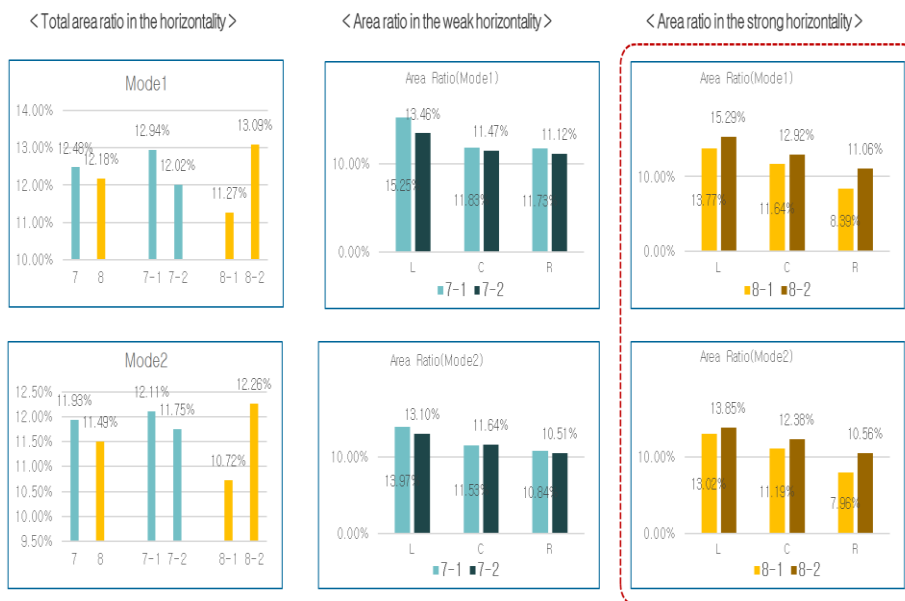


Figure 21. Results in the horizontality from welding (Test 4 - cathode)

Discussion

In test 1 (3 samples) and 3 (4 samples), the recognition efficiency of indentation according to the change in welding strength and exposure value is confirmed. As a result of the experiment, strong welding generally shows twice the results than weak welding. In addition, it can be confirmed that the higher the exposure, the lower the recognition efficiency.

In the test 2 (2 samples) and 4 (2 samples) experiments, the difference in recognition efficiency according to the location (Left, Center, Right) of the recognition area of the sample is confirmed, and as a result, the percentage of the indentation is independent of the measurement location. In other words, a sample with a large indentation area shows a larger percentage value than other samples even if Left, Center, and Right are inspected.

4. CONCLUSION

In this paper, a non-destructive inspection system for secondary battery welding was developed. The proposed system, which consists of a precision alignment stage and an imaging device that performs AOI, a non-destructive inspection, performs indentation inspection using images acquired from the camera and determines whether a product is a fake or not. The test bed was implemented and tested based on the welding, exposure, and selectable mode of the algorithm. Under the appropriate exposure, strong welding differs about twice in terms of area than weak welding and the welding can be judged by the acquired image, and in the case of strong welding, the trend according to the location can be confirmed from the experimental results according to the measurement. In particular, the proposed system showed good judgment results for the NG product, where only edges are recognized according to the mode.

REFERENCES

- [1] Alippi C, D'Angelo G, Matteucci M, Pasquettaz G, Piuri V, Scotti F. *Composite techniques for quality analysis in automotive laser welding*. Proceedings of the 2003 IEEE International Symposium on Computational Intelligence for Measurement Systems and Applications (CIMSA). Lugano. 2003; 72-77.
- [2] Stavridis J, Papacharalampopoulos A, Stavropoulos P. Quality Assessment in laser welding: a critical review. *The International Journal of Advanced Manufacturing Technology*. 2018; 94(5-8): 1825-1847.
- [3] Kim B.H., Lee D.S., Sun Lu, Chun K. GUI-based autofocusing system for AOI of FPDS. *Journal of Engineering and Applied Sciences*. 2019; 14(16): 5955-5961.
- [4] Lee D.S., Lee K.H., Chun K, Kim B.H. High definition image acquisition for automatic optical inspection using light sources characteristics. *Advanced Science Letters*. 2018; 24: 4936-4941.
- [5] Lee D.S., Lee K.H., Chun K, Kim B.H. Analysis of AOI system parameters for FOG image enhancement. *Advanced Science Letters*. 2018; 24: 4926-4930.
- [6] Lee D.S., Chun K, Kim B.H. Optimization of anisotropic conductive film bonding for improving the quality of the image in vision inspection. *International Journal of Applied Engineering Research*. 2017; 12(24): 15599-15603.
- [7] Kim B.H., Lee D.S., Lee K.H., Chun K. DIC consistent calibration for indentation mark verification in ACF images. *Journal of Engineering and Applied Sciences*. 2017; 12(Special Issue 4): 6666-6671.
- [8] Zhou G, Xu G, Gu X, Liu J. Research on evaluating laser welding quality based on two-dimensional array ultrasonic probe. *The International Journal of Advanced Manufacturing Technology*. 2016; 84(5-8): 1717-1723.
- [9] Zhang X.-G., Xu J.-J., Ge G.-Y. *Defects recognition on X-ray images for weld inspection using SVM*. Proceedings of the 2004 International Conference on Machine Learning and Cybernetics (IEEE Cat. No.04EX826). 2004; 6:3721-3725.
- [10] Wu H, Zhang X, Xie H, Kuang Y, Ouyang G. Classification of solder joint using feature selection based on Bayes and support vector machine. *IEEE Transactions on Components, Packaging and Manufacturing Technology*. 2013; 3(3): 516-522.
- [11] Wu F.-P., Zhang X.-M. Feature-Extraction-Based inspection algorithm for IC solder joints. *IEEE Transactions on Components, Packaging and Manufacturing Technology*. 2011; 1(5): 689-694.
- [12] Cai N, Lin J, Ye Q, Wang H, Weng S, Ling B. W.-K. A new IC solder joint inspection method for an automatic optical inspection system based on an improved visual background extraction algorithm. *IEEE Transactions on Components, Packaging and Manufacturing Technology*. 2015; 6(1): 161-172.